Available online at www.sciencedirect.com

ScienceDirect

Nuclear and Particle Physics Proceedings 273–275 (2016) 877–883

www.elsevier.com/locate/nppp

Searches for Higgs bosons decaying to lepton pairs with the CMS detector

Jan Steggemann for the CMS Collaboration

CERN

Abstract

Searches for Higgs bosons decaying to lepton pairs are summarised using the run 1 dataset recorded by the CMS detector. The first part of this summary is devoted to the search for Higgs bosons decaying to tau pairs. The search is carried out using all six tau-pair final states, with the tau decaying to a muon, an electron, or hadrons. Evidence for Higgs boson decays to taus is reported, and constraints on the couplings of the Higgs boson to fermions and bosons are derived. Then, searches for Higgs boson decays to muons and electrons are also discussed. The last part discusses a search for lepton-flavour violating Higgs boson decays to a muon and a tau, with the tau being reconstructed in the decay to an electron or hadrons. The analysis places the best limits on the respective Yukawa couplings to date while showing a slight excess of 2.5 standard deviations above the standard model expectation.

Keywords: Standard-model Higgs bosons, taus, lepton flavour violation

1. Introduction

At the time of the previous ICHEP conference in 2012, the discovery of a particle was reported with mass near 125 GeV and properties consistent with those of the standard model (SM) Higgs boson. While the initial and subsequent analyses measured various of the production and decay properties to be consistent with the predictions of the SM [1, 2, 3, 4, 5], measurements in different decay channels and with higher precision are necessary to probe the compatibility with the SM predictions and the mechanism of fermion mass generation. The searches for Higgs boson decays to leptons address several of the remaining open questions, most importantly whether the Higgs boson decays to fermions at all.

The first goal of the search for $H \to \tau\tau$ decays is to answer this question, i.e. to test whether the Higgs boson decays to taus, leptons, and fermions [6]. In the context of all SM Higgs boson decay modes, the $H \to \tau\tau$ final state is expected to provide the most stringent constraints on the combined couplings to fermions. The $H \to \tau\tau$ analysis also provides high sensitivity to vector boson fusion (VBF) production.

While searches for $H \to \mu\mu$ and $H \to ee$ decays are (at least currently) not sensitive to the event rates predicted by the SM, they allow to test whether the Higgs boson couplings to leptons are proportional to its mass, as predicted by the SM, or whether the couplings are flavour-universal, i.e. the same as for taus. Furthermore, $H \to \mu\mu$ decays probe the second-generation Yukawa couplings, and an enhanced $H \to \mu\mu$ decay rate may be a sign of physics beyond the SM [7].

Lepton-flavour violating (LFV) decays of the Higgs boson to leptons may occur in several extensions of the SM, e.g. in models with multiple Higgs doublets, composite Higgs models, and Randall-Sundrum models [8]. While the branching fraction to muons and electrons is severely constrained from the measurement of $\mu \to e$ transitions, $B(H \to \mu e) < O(10^{-8})$, constraints on the branching fractions $B(H \to \mu\tau)$ and $B(H \to e\tau)$ are significantly weaker, $B < O(10\%)$. The first dedicated search for $H \to \mu\tau$ decays is discussed here and is expected to significantly improve the limit on $B(H \to \mu\tau)$.

In the following, Higgs boson decay modes are always given explicitly, e.g. $H \to \tau\tau$ denotes Higgs boson decays to two taus with unspecified tau decays, and $H \to \tau\mu$ denotes the LFV direct decay of the Higgs

http://dx.doi.org/10.1016/j.nuclphysbps.2015.09.135

boson to a tau and a muon. Reconstructed lepton final states, on the other hand, are indicated by only the two final-state leptons, e.g. μe for an electron-muon final state. Reconstructed hadronic tau decays are denoted as τ_{h}. In all considered analyses, the final-state leptons are required to have opposite charge, which is therefore not explicitly noted.

This summary is organised as follows. Section 2 describes the search for $\mathrm{H} \to \tau\tau$ decays in the context of the SM. The following section 3 gives a brief overview of the searches for $\mathrm{H} \to \mu\mu$ and $\mathrm{H} \to \mathrm{ee}$ decays. Finally, the search for LFV $\mathrm{H} \to \tau\mu$ decays is reported in section 4, after which an overall summary is given.

2. Evidence for the Higgs boson decaying to a pair of taus

The branching fraction of Higgs boson decays to taus is the fourth-largest in the SM, $\mathrm{B}(\mathrm{H} \to \tau\tau) = 6.3\%$ for $m_{\mathrm{H}} = 125\,\mathrm{GeV}$. The two taus decay further and can be reconstructed in the following 6 di-tau final states in order of decreasing branching fraction, $\tau_{\mathrm{h}}\tau_{\mathrm{h}}, \mu\tau_{\mathrm{h}}, \mathrm{e}\tau_{\mathrm{h}}, \mu\mathrm{e}, \mu\mu, \mathrm{ee}$, which are accompanied by neutrinos. All 6 tau-pair final states are considered.

Events are recorded using trigger requirements based on reconstructed electron, muon, and τ_{h} candidates. The leptons are required to have low transverse momemntum (p_{T}) from nearby reconstructed photons, neutral, and charged hadrons reconstructed by the particle flow algorithm, as quantified by isolation criteria, both on trigger level and in the baseline event selection. Different p_{T} thresholds are applied for the different leptons depending on the final state and the corresponding trigger requirements. The missing transverse energy ($E_{\mathrm{T}}^{\mathrm{miss}}$) is reconstructed using a multivariate regression technique, which improves both the separation against backgrounds with high-p_{T} neutrinos and the di-tau mass reconstruction.

The relevant Higgs boson production modes for this analysis are gluon fusion, VBF, and the associated production with a W or Z boson. The different production modes are targeted by splitting the events into different categories based on the number of additional jets and leptons, and their properties. Gluon fusion production is targeted by requiring no or at least one additional jet ("0-jet/1-jet"). In the latter case, the Higgs boson may obtain a significant amount of p_{T}, thereby increasing the separation against the relevant background processes. VBF production is addressed by requiring two additional jets compatible with VBF production, i.e. with a large rapidity gap and without a central jet ("VBF tag"). Finally, the associated production with a W or Z boson is targeted by requiring one or two additional muons or electrons in the final state that are compatible with coming from a W or Z boson decay, respectively.

Additional event selection criteria are applied for a number of final states, including multivariate classifiers to separate against $\mathrm{t\bar{t}}$ background in the eμ channel and against $\mathrm{Z} \to \ell\ell$ background in the ee and $\mu\mu$ channels. To reject W+jets events, a low transverse mass $m_{\mathrm{T}} < 30\,\mathrm{GeV}$ is required in the $\mu\tau_{\mathrm{h}}$ and eτ_{h} channels.

Because of the high branching fraction, the high production cross section, and the good separation against background processes, the most important final states are $\tau_{\mathrm{h}}\tau_{\mathrm{h}}, \mu\tau_{\mathrm{h}}, \mathrm{e}\tau_{\mathrm{h}}$, and μe, in particular in the 1-jet and VBF-tag categories. In these leptonic final states, the final observable is the reconstructed di-tau mass, calculated from the two reconstructed leptons and the $E_{\mathrm{T}}^{\mathrm{miss}}$ vector. Figure 1 shows, on the one hand, the distribution of the reconstructed visible mass from the two reconstructed leptons and, on the other hand, the reconstructed mass using the so-called `SVFit` algorithm. The `SVFit` algorithm is based on a likelihood fit that takes the matrix elements for the tau decay as well as the experimental resolutions of the different input variables into account. Using the `SVFit` algorithm significantly improves the separation against the major background, $\mathrm{Z} \to \tau\tau$, and leads to an increase of the final expected significance by $\sim 40\%$ compared to using only the visible mass reconstruction.

To optimise the sensitivity of the search, the events are further divided into sub-categories to increase the separation of signal and background events using (i) the p_{T} of either the τ_{h} in final states with one τ_{h}, of the μ in the μe final state, or of the lepton with highest p_{T} in the $\mu\mu$ and ee final states, (ii) the p_{T} of the reconstructed di-tau system, and (iii) the mass of and the $\Delta\eta$ between the two jets in the VBF-tag categories.

Figure 2 shows the combined mass distribution in the four most important final states. The events are weighted by the signal over signal-plus-background ratios in a central 68% interval of the signal distributions in each event category. The figure also shows the distributions of the major backgrounds. The overall largest background is from $\mathrm{Z} \to \tau\tau$ production. It is modelled using a so-called "embedding" technique where the reconstructed muons in $\mathrm{Z} \to \mu\mu$ data are replaced by generated taus. Among the other important backgrounds are W+jets production, estimated using a control region with high transverse mass, and QCD multijet production, estimated using control regions with same-sign leptons and/or inverted lepton isolation requirements.

The final results of the analysis are obtained from a combined likelihood fit of all event categories, includ-

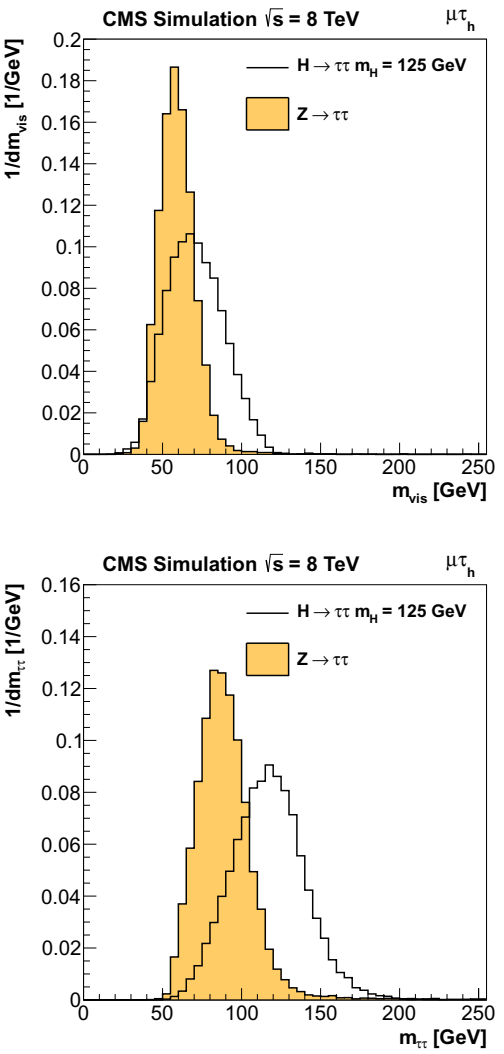

Figure 1: Top figure: Normalised distribution of the visible invariant mass of the reconstructed $\mu\tau_h$ pair in the $\mu\tau_h$ final state. Bottom figure: According distribution of the reconstructed di-tau mass using the `SVFit` algorithm.

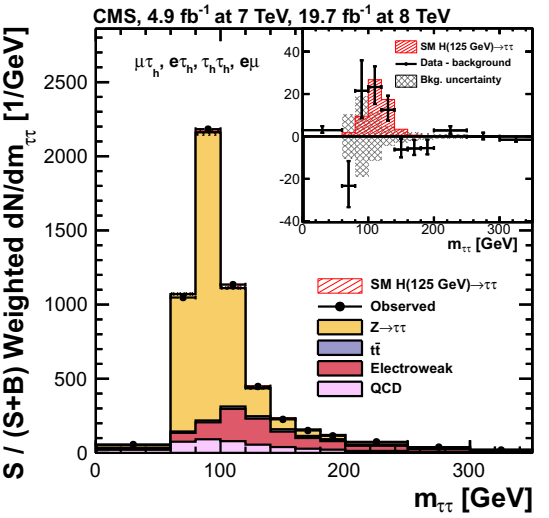

Figure 2: Combined mass distribution in the four most important final states targeting gluon fusion and VBF production. The events are weighted by the signal over signal-to-background ratio in a central 68% interval of the signal distribution in each category. The background distributions are obtained from the final combined fit.

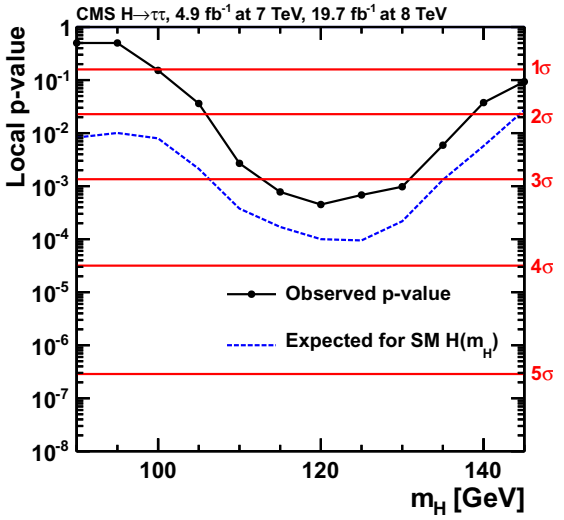

Figure 3: Observed and expected local p-values and significances in terms of standard deviations as a function of m_H.

ing all relevant systematic uncertainties. One important feature of the fit is it constrains several of the systematic uncertainties. For example, the tau energy scale and tau reconstruction efficiencies are constrained by the position and height of the Z boson mass peaks in the different lepton final states and event categories, in particular also from the distributions in the 0-jet categories that have a large contribution from $Z \to \tau\tau$ events.

The observed and expected significance of the analysis are shown in figure 3. The expected significance for $m_H = 125\,\text{GeV}$ amounts to 3.7 standard deviations (σ), and it is the highest among all m_H for two reasons. On the one hand, the mass of 125 GeV provides a better separation against the Z boson mass peak than lower m_H values. On the other hand, the cross section times branching fraction falls as as function of m_H, giving a higher expected yield than higher m_H values. The cor-

responding observed significance at 125 GeV is 3.2σ, constituting evidence for $H \to \tau\tau$ decays. To be only sensitive to $H \to \tau\tau$ decays, Higgs boson decays in the only other relevant $H \to WW$ channel are treated as a background in the calculation of the significances and best-fit signal strength modifiers in terms of the SM expectation (μ).

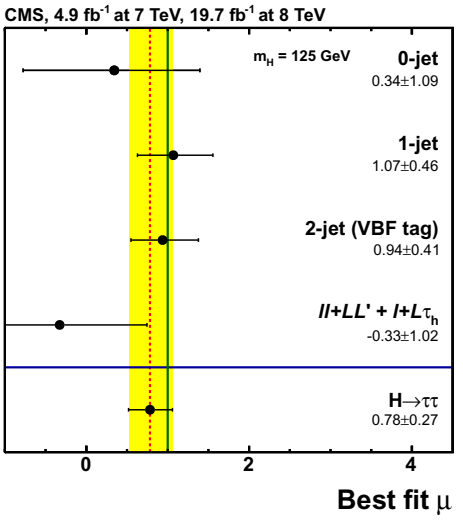

Figure 4: Measured μ values for different final states based on the number of jets and the lepton multiplicity, and combined expected and observed μ value for $m_H = 125$ GeV.

The μ values for the different jet and lepton multiplicity final states are given in figure 4. The combined best-fit μ value is 0.78 ± 0.27. Both the combined and the individual μ values are compatible with the SM expectation of $\mu = 1$. As can be seen from the uncertainties, the largest sensitivity comes from the 1-jet and VBF-tag categories.

Figure 5 shows a likelihood scan for the fermion and vector boson couplings. The parameters κ_f and κ_V denote the ratio between the measurements and SM predictions of the Higgs boson couplings to fermions and vector bosons, respectively. In this case, the contribution from $H \to WW$ is treated as a signal process. The results are compatible with the SM expectation of $\kappa_f = \kappa_V = 1$.

Finally, the results from the $H \to \tau\tau$ search are combined with a search for $H \to b\bar{b}$ [9, 10]. The combined and individual likelihood scans as a function of μ are shown in figure 6. The observed significance of the $H \to b\bar{b}$ search is 2.1σ, and the combined observed significance amounts to 3.8σ with an expectation of 4.4σ. This result constitutes strong evidence for the direct decay of the Higgs boson to fermions.

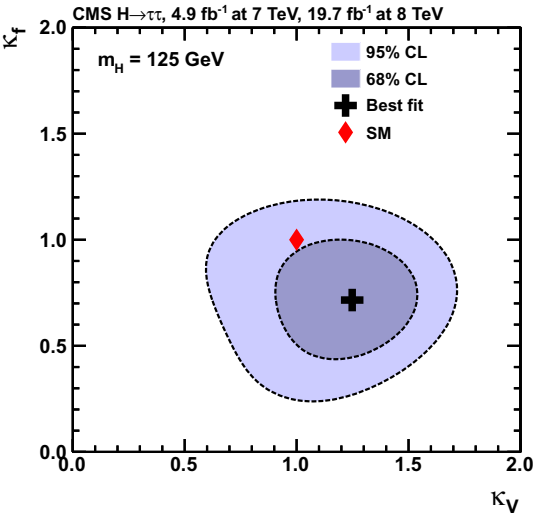

Figure 5: Likelihood scan for the combined couplings to fermions κ_f and vector bosons κ_V.

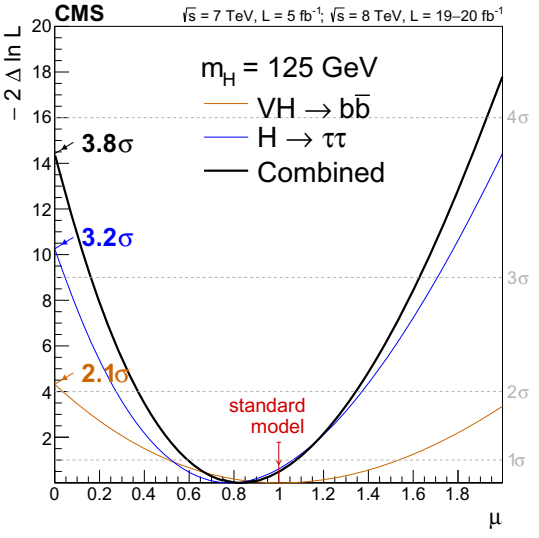

Figure 6: Likelihood scan as a function of the signal strength modifier μ for the $H \to \tau\tau$ analysis, the $H \to b\bar{b}$ analysis, and their combination.

3. Search for Higgs boson decays to muon or electron pairs

The $H \to \mu\mu$ branching fraction of 2.2×10^{-4} is among the smallest that is expected to be eventually measurable at the LHC. The $H \to \mu\mu$ search profits from

the high experimental resolution of the reconstructed di-muon mass of a few GeV [11]. However, the SM decay width of the Higgs boson is still small compared to the experimental resolution.

The analysis strategy is similar to the $H \to \tau\tau$ search. The gluon fusion and VBF production modes are targeted by requiring additional jets in the final state. In addition, the events are split into categories according to the p_T of the di-muon system, the properties of the jets in the 2-jet category, and according to the detector regions in which the two muons are reconstructed. The latter make use of the different experimental resolutions of the reconstructed di-muon mass for muons from different detector regions.

The combined di-muon mass distributions are shown in figure 7 top, weighted for the ratio of the signal and signal-plus-background distributions in the different event categories. The background distribution is estimated using an analytic fit function, and, amongst others, systematic uncertainties are estimated by changing the used fit function.

Figure 7 bottom shows the upper limits on the $H \to \mu\mu$ cross section times branching fraction in terms of the SM expectation. The combined expected limit is 5.1 times the SM expectation, while the observed 95% confidence level (CL) limit is 7.4 times the SM expectation.

For $H \to ee$, the inaccessibly small branching fraction expected in the SM is $B = 5 \times 10^{-9}$. The search follows the same strategy as the $H \to \mu\mu$ search. The resulting 95% CL upper limits on the $H \to ee$ cross section times branching fraction are shown in figure 8. They are of similar size as the limits on the $H \to \mu\mu$ cross section times branching fraction.

Contrasted with the evidence for $H \to \tau\tau$ decays, the absence of a signal in the $H \to \mu\mu$ and $H \to ee$ searches shows that the branching fraction of the Higgs boson decay to the different leptons is not identical, i.e. the decay is not universal in lepton flavour.

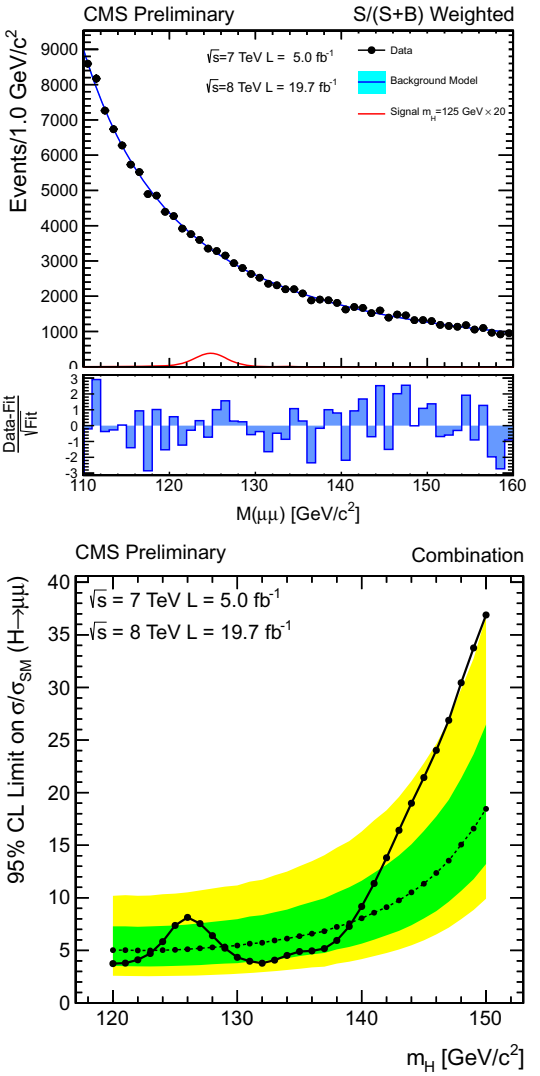

Figure 7: Top figure: Combined distribution of the reconstructed di-muon mass. The events are weighted by the ratio of the signal and signal-plus-background expectations in each individual category. Bottom figure: Upper limits on the ratio of the cross section times $B(H \to \mu\mu)$ in terms of the SM cross section times branching fraction as a function of m_H.

4. Search for LFV decays of the Higgs boson to a muon and a tau

The previous best constraints on the $H \to \tau\mu$ branching fraction are from a reinterpretation of an ATLAS $H \to \tau\tau$ search with only 7 TeV LHC data, which are more stringent than the indirect limits from $\tau \to \mu\gamma$ decays [12]. This suggests that the first dedicated search discussed here is expected to significantly improve these constraints [8]. The $H \to \tau\mu$ search considers decays of the tau to an electron or to hadron, leading to the two lepton final states $\mu\tau_h$ and μe; the $\mu\mu$ final state is not considered because of the large background from $Z \to \mu\mu$ production.

The analysis strategy is similar to the one in the search for SM Higgs boson decays to tau pairs in the corresponding $\mu\tau_h$ and μe final states. The gluon fusion production mode is targeted with two event categories requiring either 0 or 1 jet in the final state in addition to the Higgs boson decay products, and VBF production is targeted with another event category requiring two jets

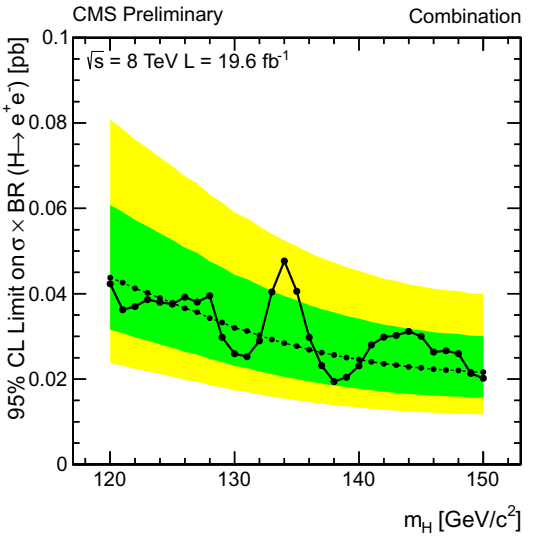

Figure 8: Upper limits on the H → ee cross section times branching fraction as a function of m_{H}.

consistent with coming from VBF production, leading to 3 event categories per lepton final state, i.e. 6 in total. Since the lepton final states are identical, the basic event selection is the same as in the two considered decay channels.

However, a number of kinematic distributions are different as the H → $\tau\mu$ decay only involves neutrinos in the decay of the tau. This implies that (a) the muon p_{T} distribution is harder than in the H → $\tau\tau$ case, (b) there is a large azimuthal angle between the muon and the sum of the neutrinos that are reconstructed as the $E_{\mathrm{T}}^{\mathrm{miss}}$ vector in the x-y plane, and (c) there is a small azimuthal angle between the visible tau decay products, i.e. either the electron or the τ_{h}, and the invisible ones being reconstructed as the $E_{\mathrm{T}}^{\mathrm{miss}}$ vector, since they originate from the same high-p_{T} tau.

To make use of these differences, additional event selection criteria are applied in each of the categories based on the p_{T} of the leptons, the differences in azimuthal angle between the final state leptons and between the electron and the $E_{\mathrm{T}}^{\mathrm{miss}}$ vector in the μe final state, and the transverse mass values calculated from either of the leptons and the $E_{\mathrm{T}}^{\mathrm{miss}}$ vector. The additional selection criteria are optimised separately in each of the 6 event categories.

As the final observable, the so-called "collinear mass" is used. Since there is only one tau in the event with high p_{T} compared to its mass, the approximation is made that the neutrino momenta, measured as the $E_{\mathrm{T}}^{\mathrm{miss}}$ vector, and the momenta of the visible tau decay products are in the same direction as the tau momentum.

The backgrounds are also estimated with similar methods as in the SM H → $\tau\tau$ search. Due to the tighter event selection, two important differences arise. First, the Z → $\tau\tau$ can be suppressed more efficiently, meaning that other sources of background are most relevant, in particular W+jets, multijet, and $\mathrm{t\bar{t}}$ events. Second, due to this suppression, the 0-jet categories also provide high sensitivity.

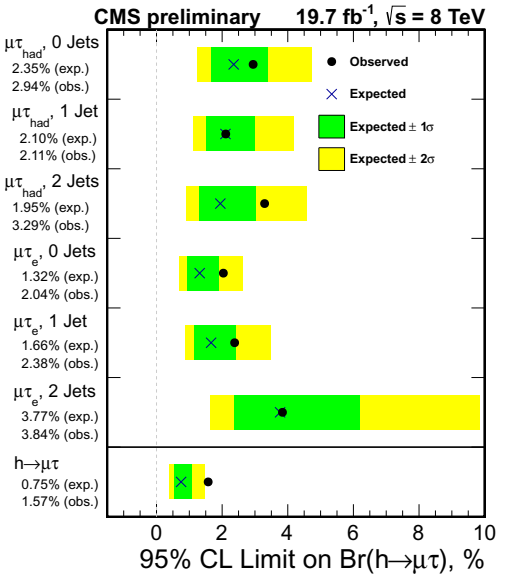

Figure 9: Upper limits on the branching fraction of LFV H → $\tau\mu$ decays. The limits are shown separately for the 6 different event categories and their combination.

Upper limits on the branching fraction of H → $\tau\mu$ decays are obtained with the $\mathrm{CL_S}$ method using a combined likelihood fit. The resulting limits are shown in figure 9, both for the 6 event categories and their combination. The expected upper limit on the H → $\tau\mu$ branching fraction is 0.75%, while the observed limit is 1.57%. With respect to the background-only expectation, a slight excess is observed. The background-only p-value is 0.007 for m_{H} = 126 GeV, corresponding to a significance of 2.5σ. The best-fit branching fraction is measured to be $\mathrm{B(H} \to \tau\mu) = (0.89^{+0.40}_{-0.37})\%$.

Finally, the results are translated into limits on the flavour-violating Yukawa couplings, $|Y_{\mu\tau}|$ and $|Y_{\tau\mu}|$, as shown in figure 10. The presented search improves the previous best limits on the Yukawa couplings by an order of magnitude.

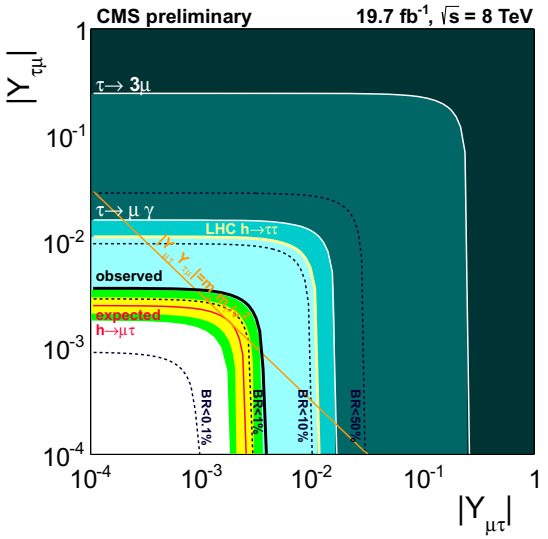

Figure 10: Constraints on the flavour-violating Yukawa coupling $Y_{\mu\tau}$, with the expected limits given by the red line and the observed limits as the full black line. The previous best direct experimental limits from $\tau \to \mu\gamma$ decays are given by the white line and the middle blue-green area, and the limits from a re-interpretation of an ATLAS $H \to \tau\tau$ search are drawn as a yellow line.

5. Conclusion

In the search for $H \to \tau\tau$ decays, evidence for Higgs boson decays to tau pairs is obtained, with an observed significance of 3.2 standard deviations given an expectation of 3.7 standard deviations. The measured event rates, mass, and couplings to fermions and vector bosons are consistent with expectations from the SM. The combination with the search for Higgs boson decays to b quarks yields strong evidence for Higgs boson decays to fermions. Tight constraints are also derived on the $H \to \mu\mu$ and $H \to$ ee branching fractions, showing that the Higgs boson couplings to leptons are not flavour-universal.

The search for LFV provides the most stringent limits $H \to \tau\mu$ decays and the $Y_{\tau\mu}$ Yukawa coupling to date. Results with LHC run 2 data will resolve whether the slight excess that is observed can be attributed to a statistical fluctuation.

References

[1] ATLAS Collaboration, Observation of a new particle in the search for the Standard Model Higgs boson with the ATLAS detector at the LHC, Phys. Lett. B 716. arXiv:1207.7214, doi:10.1016/j.physletb.2012.08.020.

[2] CMS Collaboration, Observation of a new boson at a mass of 125 GeV with the CMS experiment at the LHC, Phys. Lett. B 716. arXiv:1207.7235, doi:10.1016/j.physletb.2012.08.021.

[3] CMS Collaboration, Observation of a new boson with mass near 125 GeV in pp collisions at $\sqrt{s} = 7$ and 8 TeV, JHEP 06 (2013) 081. doi:10.1007/JHEP06(2013)081.

[4] CMS Collaboration, Study of the Mass and Spin-Parity of the Higgs Boson Candidate via Its Decays to Z Boson Pairs, Phys. Rev. Lett. 110 (2013) 081803. arXiv:1212.6639, doi:10.1103/PhysRevLett.110.081803.

[5] ATLAS Collaboration, Evidence for the spin-0 nature of the Higgs boson using ATLAS data, Phys. Lett. B 726 (2013) 120. arXiv:1307.1432, doi:10.1016/j.physletb.2013.08.026.

[6] CMS Collaboration, Evidence for the 125 GeV Higgs boson decaying to a pair of τ leptons, J. High Energy Phys. 05 (2014) 104. doi:10.1007/JHEP05(2014)104.

[7] A. Dery, A. Efrati, Y. Hochberg, Y. Nir, What if BR(H $\to \mu\mu$)/BR(H $\to \tau\tau$) does not equal m_μ^2/m_τ^2?, JHEP 05 (2013) 039. arXiv:1302.3229, doi:10.1007/JHEP05(2013)039.

[8] CMS Collaboration, Search for Lepton Flavour Violating Decays of the Higgs Boson, CMS Physics Analysis Summary CMS-PAS-HIG-14-005 (2014).
URL `http://cds.cern.ch/record/1740976`

[9] CMS Collaboration, Search for the standard model Higgs boson produced in association with a W or a Z boson and decaying to bottom quarks, Phys.Rev. D89 (1) (2014) 012003. arXiv:1310.3687, doi:10.1103/PhysRevD.89.012003.

[10] CMS Collaboration, Evidence for the direct decay of the 125 GeV Higgs boson to fermions, Nature Phys. 10. doi:10.1038/nphys3005.

[11] CMS Collaboration, Search for standard model Higgs boson production in the $\mu^+\mu^-$ final state with the CMS experiment in pp collisions at $\sqrt{s} = 7$ and 8 TeV, CMS Physics Analysis Summary CMS-PAS-HIG-13-007 (2013).
URL `http://cdsweb.cern.ch/record/1606831`

[12] R. Harnik, J. Kopp, J. Zupan, Flavor Violating Higgs Decays, JHEP 03 (2013) 026. arXiv:1209.1397, doi:10.1007/JHEP03(2013)026.